Pergamon

Geochimica et Cosmochimica Acta, Vol. 68, No. 5, pp. 949–958, 2004

0016-7037/04 $30.00 + .00

doi:10.1016/j.gca.2003.07.002

Oxygen isotope exchange kinetics between H_2O and H_4SiO_4 from ab initio calculations

MIHALI A. FELIPE,*,[1] JAMES D. KUBICKI,[2] and DANNY M. RYE[1]

[1]Department of Geology and Geophysics, Yale University, New Haven, CT 06511 USA
[2]Department of Geosciences, The Pennsylvania State University, University Park, PA 16802, USA

(*Received December* 9, 2002; *accepted in revised form July* 24, 2003)

Abstract—Oxygen isotope exchange between H_2O and H_4SiO_4 was modeled with ab initio calculations on H_4SiO_4 + $7H_2O$. Constrained optimizations were performed with the B3LYP/6-31+G(d,p) method to determine reactants, transition states, and intermediates. Long-range solvation was accounted for using self-consistent reaction field calculations. The mechanism for exchange involves two steps, a concerted proton transfer from H_4SiO_4 forming a 5-coordinated Si followed by a concerted proton transfer from the 5-coordinated Si forming another H_4SiO_4. The 5-coordinated Si intermediate is C2 symmetric. At 298K and with implicit solvation included, the Gibbs free energy of activation from transition state theory is 66 kJ/mol and the predicted rate constant is 16 s^{-1}. Equilibrium calculations between 298K and 673K yield $\alpha_{H4SiO4\text{-}H2O}$ that are uniformly less than, but similar to, $\alpha_{qtz\text{-}H2O}$, and therefore $\alpha_{qtz\text{-}H4SiO4}$ is expected to be relatively small in this temperature range.

1. INTRODUCTION

The composition of oxygen isotopes in silicates is dependent on their genesis and history. Therefore, the mechanisms of oxygen exchange between the different interacting species in natural systems should be well understood before an overall picture of the kinetics of mineral-water exchange can be made. One of these interacting species is orthosilicic acid or H_4SiO_4. There has been debate on whether H_4SiO_4 is the predominant silicon species in solution, although it is generally recognized that it is present when silicates are dissolved (Dove and Rimstidt, 1994; Zotov and Keppler, 2002); and thus, it is an important aqueous phase Si species. Aqueous H_4SiO_4 may precipitate out of solution producing solid silica or be biologically assimilated forming tests of organisms such as diatoms or plant phytoliths. Therefore, understanding the oxygen isotope exchange between aqueous H_4SiO_4 and water has various applications that include quartz-water exchange (Clayton et al., 1988, 1989; Chiba et al., 1989), biogenic silica in paleothermometry (Knauth, 1994; Schmidt et al., 1997; Brandriss et al., 1998; Barker et al., 2001; Shemesh et al., 2001; Schmidt et al., 2001) and paleoclimate studies (Webb and Golding, 1998; Webb and Longstaffe, 2000), and petroleum reservoir analysis (Williams et al., 1997).

The reaction $SiO_2 + 2H_2O \rightarrow H_4SiO_4$ (e.g., Rimstidt and Barnes, 1980) suggests that as silica dissolves, the mean oxygen isotopic signature of the aqueous orthosilicic acid formed would be derived from the initial silica and the aqueous solution in equal proportions. Once $H_4SiO_{4(aq)}$ has formed however, oxygen isotope exchange between the orthosilicic acid and solvent is possible. Indeed, most studies of oxygen isotopes in precipitated silicates assume that the isotopic value reflects the ambient value in the water rather that a mixture of silicate and water values (e.g., Lasaga and Rye, 1993; Jenkin et al., 1994; Brandriss et al., 1998; Cole 2000; Gotze, 2001; Jia et al., 2001). This assumption implies that the rate of oxygen isotope exchange between water and orthosilicic acid is relatively fast.

Oxygen exchange rates as inferred from NMR studies of the silicate dimerization/hydrolysis (Kinrade, 1996; Swaddle, 2001) show that it is fast through this mechanism (rate constant of 3.8 s^{-1} at 298K). However, this would imply that the rate is driven by the transport of orthosilicic acid and is a second-order function of the silicate concentration; the latter implication has not been demonstrated experimentally. On the other hand, the direct exchange of oxygen between water and orthosilicic acid would be driven by the transport of water and would be first-order with respect to orthosilicic acid concentration. Research into the rate and mechanism of direct oxygen isotope exchange between water and orthosilicic acid specifically has not been conducted to our knowledge.

Some related studies have addressed the issue of oxygen exchange between water and other species such as dissolved Al(III) complexes (Casey et al., 2000; Phillips et al., 2000; Casey and Phillips, 2001; Lee et al., 2002), surface species of SiO_2, Al_2O_3, ZrO_2, MgO, CeO_2 (Martin and Duprez, 1996), and complexes of Cr(VI) (Brasch et al., 1996). Although it has been shown that empirically measured rates may correlate with theoretically derived parameters such as charges or bond lengths, one of the reasons for conducting a complete transition state analysis of the H_4SiO_4-H_2O system is that an outcome of these studies is a complete temperature-dependent equation for the rate constants that may be evaluated at any temperature. Temperature-dependent equations are useful, for example, in advection-diffusion-reaction or mass transfer computations (e.g., Bolton et al., 1999) where reactions are evaluated along a temperature gradient. Another reason for conducting these studies is that the decomposition of reactions into their elementary mechanisms provides the resolution to quantitatively evaluate long-held models (e.g., Knight et al., 1989) and if possible improve on them. In this work, we begin to develop a methodology for modeling oxygen isotope exchange with ab initio calculations. This work is a step towards elucidating the nature of the H_4SiO_4-H_2O system in general.

The H_4SiO_4-H_2O system was chosen because of its applica-

* Author to whom correspondence should be addressed (mihali@aya.yale.edu).

tions as discussed above and its amenability to quantum cluster calculations (Pelmenschikov et al., 1997; Kubicki, 2001). Experimental studies of the oxygen isotope exchange rate should also be practical; hence, we hope to prompt investigations of this type to test our predictions. From work on a relatively simple system such as H_4SiO_4-H_2O, it will be possible to later extend similar ab initio studies to polymerized silicates in solution (Iler, 1979), to other species with slower O-exchange rates (e.g., PO_4^{3-}, SO_4^{2-}) and to reactions with mineral surfaces (Casey, 2001).

2. THEORY

In this study, we make use of MO-TST as described in Felipe et al. (2001, 2003) to determine activation energies and rate constants for $H_4SiO_4 + 7H_2O$, which was chosen to represent dissolved silica in water. By treating the systems as unimolecular and assuming a polyatomic ideal gas, the forward rate constant can be expressed as

$$k_f = \frac{k_B T}{h} \exp\left(\frac{-\Delta G^{\ddagger}}{N_A k_B T}\right) \tag{1}$$

where k_B is Boltzmann's constant, T is the temperature, h is Planck's constant, $\Delta G^{\ddagger}$ is the free energy change from reactants to the transition state, and N_A is Avogadro's number. Thermodynamics gives $\Delta G^{\ddagger} = \Delta E^{\ddagger} - T\Delta S^{\ddagger} + p\Delta V^{\ddagger}$ where $\Delta E^{\ddagger}$, $\Delta S^{\ddagger}$ and $\Delta V^{\ddagger}$ are the internal energy, entropy and volume changes, respectively, from reactants to the transition state. The quantity $\Delta E^{\ddagger}$ is the zero-point energy corrected barrier (ZPECB or ΔE_o) in Felipe et al. (2003). Statistical mechanics relates the pressure p and entropy S to the partition functions q by

$$p = k_B T\left(\frac{\partial \ln q}{\partial V}\right)_{N,T} \tag{2}$$

$$S = k_B \ln q + k_B T\left(\frac{\partial \ln q}{\partial T}\right)_{N,V} \tag{3}$$

Eqn. 1 is equivalent to $k = (k_{BT}/h)Q^{\ddagger}/Q \exp(\Delta\varepsilon_o/k_{BT})$ but emphasizes the resolution to different thermodynamic contributions, where Q is the partition function and $\Delta\varepsilon_o$ is the difference in zero-point energies. This emphasis is useful because significant errors may be introduced in the entropy if the harmonic approximation is used to calculate the partition function for low frequency modes that represent hindered internal rotation (East and Radom, 1997; Ayala and Schlegel, 1998). Hence, rather than rely on a cancellation of errors between reactants and transition states, or on identifying and individually treating internal rotational modes, one may as a way to minimize errors opt to disregard S_{vib} in computing $\Delta G^{\ddagger}$. Thus, two sets of $\Delta G^{\ddagger}$ and reaction rate constants would be presented, one in which $S_{vib} = 0$ (hence, $\Delta S^{\ddagger}_{vib} = 0$) and another with the full $S_{vib} \neq 0$ (hence, $\Delta S^{\ddagger}_{vib} \neq 0$). The former would be considered more accurate of the two sets of data.

Calculated vibrational frequencies and zero-point energies systematically vary with the MO method. Hence, scaling factors need to be incorporated for frequencies and zero-point energies to be comparable with empirical data (Pople et al., 1993; Scott and Radom, 1996). Scaling factors express themselves as coefficients to the vibrational frequencies and concomitantly the zero-point energy corrections. A scaling factor of 0.96 for all vibrational frequencies (Foresman and Frisch, 1996) was used in the calculation of p, S, G and thus equilibrium and rate constants.

System solvation was treated using explicit and implicit hydration. Explicit hydration is accomplished by adding discrete numbers of water molecules to the system. For the implicit hydration, the integral equation formalism polar continuum model (IEFPCM) of Cancès et al. (1997) was used. Hence, with the IEFPCM model, $\Delta G^{\ddagger}$ in Eqn. 1 is replaced by $\Delta G^{\ddagger}_{solv}(T)$

$$\Delta G^{\ddagger}_{solv}(T) = \Delta G^{\ddagger} + \varepsilon^{\ddagger}_{solv}(T) - \varepsilon_{rct,\,solv}(T) \tag{4}$$

where $\varepsilon^{\ddagger}_{solv}(T)$ and $\varepsilon_{rct,solv}(T)$ are transition state and reactant solvation free energy corrections.

In many cases, it is worthwhile to relate computed kinetic parameters to measured thermodynamic quantities. We compute the equilibrium constant for an elementary reaction directly using

$$K_{eq} = \exp\left(\frac{-\Delta G^{o}}{N_A k_B T}\right) \tag{5}$$

where ΔG^o is the free energy change from reactants to products. Fractionation factors for isotope exchange reactions (O'Neil 1986) can be computed as well, using the following relationship between α and K_{eq}

$$\alpha = K_{eq}^{1/x} \tag{6}$$

where the number of isotopes exchanged x = 1. Because x is unity in Eqn. 5, we shall use the term "equilibrium constant" and "fractionation factor" interchangeably.

3. METHODOLOGY

Ab initio calculations were carried out using gaussian 98 (Frisch et al., 1998) on an Intel Pentium III running Linux 2.2, and using gaussian 94 (Frisch et al., 1995) on a DEC Alpha 600au and on two DEC Alpha XP1000's running Compaq Tru64 UNIX. A density functional theory with hybrid functionals method, in particular Becke's three-parameter method (Becke, 1993) with Lee-Yang-Parr functionals (Lee et al., 1988) or B3LYP, was used to account for electron exchange and correlation. Extended and diffuse basis sets 6-31G(d) and 6-31+G(d,p) (Hehre et al., 1972) were used to build the singlet state electron wave functions of the molecular configurations. Optimizations were performed in these levels using the optimized result from the lower level as input for the higher level.

Local energy minima within the vicinity of the starting and ending configurations were sought using standard methods as outlined by Peng and Schlegel (1994). These potential energy minima correspond to prospective reactants, products and intermediates of the reactions of interest. Having computed the local minima, the first-order saddle points that link them were then sought. These first-order saddle points correspond to the transition states of reaction mechanisms and are similar to energy minima except a slight change along one particular direction lowers the energy. This direction is the reaction coordinate. A complete reaction mechanism is defined by a pair

of local minima (reactants, and products or intermediates) and a first-order saddle point (transition state) linking the two.

Seven water molecules were chosen because odd numbers of water molecules can be made to produce symmetric 5-coordinated intermediates as water approaches the silicon center. Preliminary calculations on three and five water molecule systems (see for example, Felipe et al., 2001) have failed to yield an optimized transition state at the desired level of theory. There were no symmetry constraints imposed in any of the calculations. The 5-coordinated minimum makes an ideal isotope exchange intermediate because protonation of one hydroxide represents a water molecule leaving-group and the transfer of the hydrogen to another hydroxide group represents another water molecule leaving-group. Silica has a local energy minimum in a 5-coordinated configuration (Kubicki et al., 1993; Xiao and Lasaga, 1996), and the stability of this configuration depends on solvation (Sefcik and Goddard, 2001). However, the direct involvement of surrounding water molecules needs to be further investigated.

A C2 symmetric 5-coordinated local energy minimum was used as a starting configuration for the succeeding reaction coordinate searches. This minimum has a water molecule in the equatorial position and makes it an ideal candidate for an intermediate in an oxygen isotope-exchange reaction because drawing out either of the axial position oxygen atoms would yield half of a possible isotope exchange reaction. The arrangement of molecules is such that the transfer of protons is facilitated via two mediating water molecules. Thus, we could verify whether the known ease of which protons transfer in water (Luth and Scheiner, 1992; Lobaugh and Voth, 1996; Geissler et al., 2001; Felipe et al., 2003) possibly enhances the rate of the oxygen isotope exchange reaction. Xiao and Lasaga (1994) have already computed the ZPCEB for proton transfer without a mediating water molecule, that is, the direct transfer of the proton from one hydroxide to another, so results can be compared with this previous work.

In these calculations, problems such as basis-set superposition errors (BSSE; Sauer, 1989) and size consistency (Hehre et al., 1986) were minimal because all energy differences were computed using reactant, transition-state and product configurations that have the same stoichiometry and similar structures. The reactions were treated unimolecularly and the constituent molecules were never treated as isolated entities. Therefore, these calculations make use of the same basis set and the same number of basis functions with minimal basis set superposition differences. Furthermore, corrections suggested in the literature such as the counterpoise method (Boys and Bernardi, 1970) are approximations and may overestimate BSSE and eventually lead to a larger error than not making corrections at all (H. B. Schlegel, private communication). However, BSSE can play a significant role in the structure and energy of transition state calculations (e.g., Kobko and Dannenberg, 2001).

Transition state configurations were computed using the methods discussed in Felipe et al. (2003). Searches were aborted when the energy difference between the constrained configuration and the nearest local minimum exceeded 100 kJ/mole, which is an arbitrarily set threshold. After calculating the three configurations representing reactant, product and transition-state, vibrational analyses were performed to correct for zero-point energies. These calculations assume that the energy within the system is in the form of vibrations along normal modes. This is a reasonable approximation for simulations of condensed state reactions (see Drenth and Kwart, 1980).

There are numerous position permutations of orthosilicic acid and multiple water molecules. Therefore, it is expected that other paths by which isotope exchange occurs possibly exist. Hence, it is not claimed that the path described here is definitely the rate determining one. We hypothesize, however, that any competing path should kinetically be faster than this path to be significant contributors to the rate; the path that we present is therefore perceived to represent lower bounds to the rate (i.e., the true k_f could only be greater or equal to what we compute).

4. RESULTS AND DISCUSSION

4.1. Mechanism

The full reaction mechanism is shown in Figure 1 with selected interatomic distances listed in Table 1. Oxygen isotope exchange was facilitated by a concerted transfer of protons similar to the hydrogen isotope exchange of Felipe et al. (2003). The mechanism involved two elementary reactions (i.e., two steps). The atoms directly participating in the reaction are numbered (1) to (13). Henceforth, numeric labels of atoms will be indicated by subscripts in square brackets, e.g., $O_{[1]}$. The participating atoms were in an H-bonding network with H-bonds ranging from 1.71 to 2.02 Å. This is a common range for H-bonding in water (see Keutsch and Saykally, 2001, for a recent review).

The reactant (Fig. 1a) H_4SiO_4 has normal Si-O bond lengths of (1.63 and 1.68 Å Si-$O_{[7,13,14,15]}$, that is the distance of Si from O labeled 7, 13, 14 and 15) in agreement with that predicted by Newton and Gibbs (1980), McMillan and Hess (1990) and De Almeida and O'Malley (1991) and the variation is within the expected range of vibrational stretching. In the reactant configuration, $O_{[1]}$ of the incoming water molecule has a distance of 3.64 Å from the silicon atom. This is similar to other hydrating H_2O molecules in the configuration (3.54 to 3.81 Å). Frequency calculations on the configuration in Figure 1a verify that this is an energy minimum. The configuration of the H_4SiO_4 is close to tetrahedral with $O_{[7,14,15]}$-Si-$O_{[13]}$ angles ranging from 106.8° to 110.3°.

The configuration shown in Figure 1b is a sample step between the reactant and the first transition state. The Si-$O_{[1]}$ distance was constrained to 2.30 Å. This configuration was chosen to illustrate configurations between the reactant (Si-$O_{[1]}$ distance of 3.64 Å) and the transition state (Si-$O_{[1]}$ distance of 1.88 Å, see Fig. 1c). Note that the Si-$O_{[13]}$ distance has lengthened to 1.71 Å, whereas the H-O bonds in the vicinity of the incoming H_2O are slightly shorter (0.99 Å for $O_{[1]}$-$H_{[2]}$ and $O_{[3]}$-$H_{[4]}$). These show that caution should be taken when interpreting bond length changes, especially when they are used as indicators of how a reaction would eventually proceed. The configuration of the H_4SiO_4 is between a tetrahedral and trigonal bipyramidal with $O_{[7,14,15]}$-Si-$O_{[13]}$ angles ranging from 96.7° to 103.5°.

Figure 1c shows the first transition state of the reaction. Vibrational analysis on the configuration yields one imaginary frequency and visual inspection of the configuration changes in

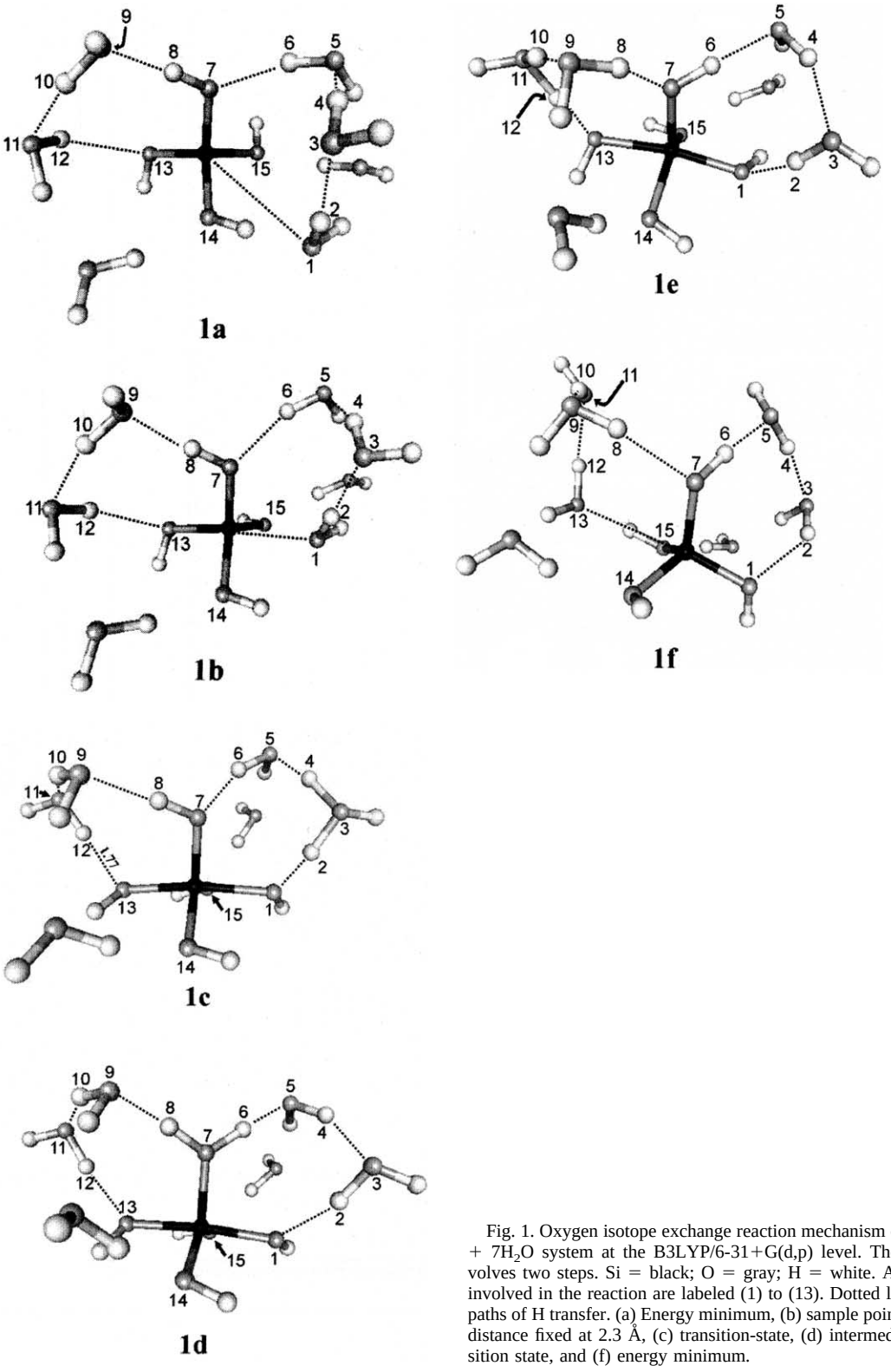

Fig. 1. Oxygen isotope exchange reaction mechanism of the H_4SiO_4 + $7H_2O$ system at the B3LYP/6-31+G(d,p) level. The reaction involves two steps. Si = black; O = gray; H = white. Atoms directly involved in the reaction are labeled (1) to (13). Dotted lines represent paths of H transfer. (a) Energy minimum, (b) sample point with Si-$O_{[1]}$ distance fixed at 2.3 Å, (c) transition-state, (d) intermediate, (e) transition state, and (f) energy minimum.

the direction of steepest descent show that this corresponds to the desired reaction. Observe that the Si-$O_{[1]}$ distance has decreased to 1.88 Å and the Si-$O_{[13]}$ distance is increased to 1.76 Å. In comparison, the distances between the central Si to the now equatorial oxygen atoms are shorter (Si-$O_{[7,14,15]}$ bond distances of 1.67 to 1.73 Å). $H_{[2]}$ is in the process of transferring from $O_{[1]}$ to $O_{[3]}$; the role of explicit hydration is critical because proton transfer cannot occur if only a single H_2O

Table 1. Selected interatomic distances in angstroms.[a]

Atoms	1a	1b	1c‡	1d	1e‡	1f
$0_{[1]}$-$H_{[2]}$	1.00	0.99	1.32	1.77	1.77	2.02
$H_{[2]}$-$O_{[3]}$	1.71	1.72	1.12	0.99	0.99	0.98
$O_{[3]}$-$H_{[4]}$	1.00	0.99	1.18	1.81	1.89	1.82
$H_{[4]}$-$O_{[5]}$	1.72	1.76	1.25	0.98	0.98	0.99
$O_{[5]}$-$H_{[6]}$	0.98	0.98	1.01	1.44	1.70	1.59
$H_{[6]}$-$O_{[7]}$	1.91	1.90	1.64	1.05	1.00	1.02
$O_{[7]}$-$H_{[8]}$	1.02	1.00	1.00	1.05	1.64	1.91
$H_{[8]}$-$O_{[9]}$	1.59	1.65	1.70	1.44	1.01	0.98
$O_{[9]}$-$H_{[10]}$	0.99	0.99	0.98	0.98	1.25	1.72
$H_{[10]}$-$O_{[11]}$	1.82	1.73	1.89	1.81	1.18	1.00
$O_{[11]}$-$H_{[12]}$	0.98	0.97	0.99	0.99	1.12	1.71
$H_{[12]}$-$O_{[13]}$	2.02	2.02	1.77	1.77	1.32	1.00
Si-$O_{[1]}$	3.64	2.30	1.89	1.77	1.76	1.67
Si-$O_{[7]}$	1.63	1.64	1.68	1.74	1.68	1.63
Si-$O_{[13]}$	1.67	1.71	1.76	1.77	1.89	3.64
Si-$O_{[14]}$	1.63	1.68	1.71	1.72	1.72	1.68
Si-$O_{[15]}$	1.68	1.69	1.72	1.72	1.71	1.63

[a] The double dagger superscript (‡) indicates a transition state.

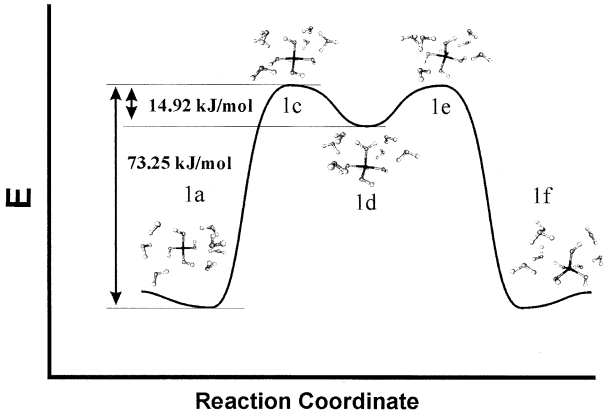

Fig. 2. Schematic diagram of ZPECB showing values for the zero net isotope exchange reaction. If ^{18}O is substituted into $O_{[1]}$, the barrier height from 1a to 1c becomes 73.17 kJ/mol while the barrier height from 1f to 1e becomes 73.24 kJ/mol.

molecule attacks H_4SiO_4. Concurrent with the proton transfer is the formation of the $H_3O^+ \cdots H_2O$ dimer. The $O_{[3]}$-$H_{[4]}$ and $H_{[4]}$-$O_{[5]}$ distances are similar and they are longer than ordinary O-H distances. Note that the model is effectively an ion-pair where we have formed a positively charge $H_3O^+ \cdots H_2O$ and a negatively charged $H_5SiO_5^-$. This ion pair formation can affect the H-bonding to the solute. The decrease in distance between $H_{[6]}$ and $O_{[7]}$ (1.91 to 1.68 Å) is noteworthy because it evinces the eventual transfer of $H_{[6]}$ to $O_{[7]}$ to form a reaction intermediate.

Figure 1d is a C2-symmetric trigonal bipyramidal intermediate. The transfer of $H_{[6]}$ to $O_{[7]}$ effectively creates an H_2O group in the equatorial position of the trigonal bipyramid. Bond distances of axial bonds Si-$O_{[1]}$ and Si-$O_{[13]}$ are the same (1.77 Å). The Si-$O_{[7]}$ distance is slightly longer than the two other equatorial bonds, Si-$O_{[14,15]}$. The $H_{[6]}$ to $O_{[5]}$ and $H_{[8]}$ to $O_{[9]}$ distances (both 1.44 Å) are small for hydrogen bonding and suggest that transfer of the proton can easily be accomplished. Frequency calculations on the configuration in Figure 1d verify that this is an energy minimum.

The symmetry of the intermediate shown in Figure 1d indicates that the other axial oxygen, that is $O_{[13]}$, is equivalent to $O_{[1]}$. Thus, $O_{[13]}$ may leave the Si centered complex in exactly the opposite way that $O_{[1]}$ approached the central Si. Figures 1e and 1f are, respectively, the optimized transition state and energy minimum configurations of the $O_{[13]}$ leaving the Si center eventually forming a water molecule on the other side of the H_4SiO_4 (compare Figs. 1a with 1f). By substituting ^{18}O with either $O_{[1]}$ or $O_{[13]}$, a complete reaction mechanism for the oxygen isotope exchange reaction has been illustrated.

Table 2. Zero-point corrected absolute energies of configurations used in this study.[a]

		6–31G(d)	6–31+G(d,p)
$H_4SiO_4 + H_2{}^{18}O + 6H_2O$	[1a]	−1127.786198	−1127.952565
[TS1]	[1c]	−1127.760645	−1127.924692
$H_6SiO_4{}^{18}O + 6H_2O$	[1d]	−1127.762090	−1127.930375
[TS2]	[1e]	−1127.760644	−1127.924694
$H_4SiO_3{}^{18}O + 7H_2O$	[1f]	−1127.786219	−1127.952595
$H_4SiO_4 + 7H_2O$	[1a or 1f]	−1127.786072	−1127.952437
[TS]	[1c or 1e]	−1127.760498	−1127.924531
$H_6SiO_5 + 6H_2O$	[1d]	−1127.761943	−1127.930215

[a] All configurations are computed using B3LYP. Units are in hartrees (1 hartree = 2625 kJ/mol).

The reaction depicted here shows that H_2O plays a key role in the isotope exchange by facilitating the transfer of protons. Previous calculations by Xiao and Lasaga (1994) have shown that the direct transfer of protons from one OH group of H_4SiO_4 to another has a large energy barrier. Furthermore, studies with only a few water molecules (e.g., Casey et al., 1990; Xiao and Lasaga, 1994) predict a large H/D kinetic isotope effect that is not observed experimentally. Hence, discrepancies between theory and experiment may be minimized by eliminating possible artifacts introduced by neglecting treatment of the solvating water molecules.

Aside from the reaction mechanism described in Figure 1 and the discussion above, we have attempted to find alternative paths starting from 1d. Pulling out the equatorial H_2O by constraining the Si-$O_{[7]}$ distance, and constraining the $O_{[7]}$-Si-$O_{[14]}$ angle to make the equatorial oxygen atoms axial, yield energy barriers about twice higher than the energy difference between 1d and 1b (and similarly 1d and 1e). These alternative paths are less energetically favored than the mechanism presented in Figure 1.

The system is electronically neutral and favors the availability of protons to facilitate the exchange reaction. In the bulk system therefore, it is expected that a higher pH would limit the number of such configurations and thus retard the exchange through this particular mechanism. The pH dependence is similar to the oxygen exchange mechanism of Kinrade (1996) where the reaction is a consequence of the dimerization and hydrolysis of silica, that is both mechanisms require the availability of Si-OH groups.

4.2. Zero-Point Energy Corrected Barriers and Free Energies of Activation

Table 2 lists the absolute energies of the configurations, and Figure 2 schematically shows the ZPECBs. We shall refer to

Table 3. Solvation corrected Gibbs free energies from IEFPCM and B3LYP/6–31+G(d,p).[a]

T(K)	298	373	473	573	673
p(Mpa)	0.1	1.0	5.0	22	100
Diel	78.54	50.0	38.0	26.0	15.0
$S_{vib} = 0$:					
1a	−1127.946245	−1127.934571	−1127.917709	−1127.899117	−1127.878377
1c	−1127.921047	−1127.910031	−1127.893858	−1127.875803	−1127.855568
1d	−1127.925639	−1127.914243	−1127.897655	−1127.879265	−1127.858684
1e	−1127.921046	−1127.910029	−1127.893855	−1127.875801	−1127.855565
1f	−1127.946271	−1127.934591	−1127.917722	−1127.899124	−1127.878380
$S_{vib} \neq 0$:					
1a	−1128.027211	−1128.045604	−1128.074476	−1128.105793	−1128.138185
1c	−1127.994462	−1128.010912	−1128.037009	−1128.065445	−1128.094976
1d	−1128.002239	−1128.019518	−1128.046828	−1128.076553	−1128.107362
1e	−1127.994464	−1128.010914	−1128.037013	−1128.06545	−1128.094983
1f	−1128.027217	−1128.045606	−1128.074474	−1128.105788	−1128.138178

[a] Data are presented in units of hartrees (1 hartree = 2625 kJ/mol).

the configurations shown in Figure 1 by their corresponding letter, e.g., "1a" would mean "the configuration shown in Figure 1a."

In the absence of isotopic changes, the zero-point corrected PES would be symmetric. For the zero net isotopic exchange reaction, the ZPECB from 1a (or 1f) to 1d is 73.25 kJ/mol and from 1d to 1a (or 1f) is 14.92 kJ/mol. (The values listed here are given four significant figures to show the magnitude of energy changes but do not necessarily imply that the values are accurate to 0.01 kJ/mol.) On the other hand, substitution of ^{18}O in $O_{[1]}$ changes the zero point corrected absolute energies and hence changes the ZPECBs because the symmetry of the zero-point corrected PES is broken. With $^{18}O_{[1]}$, the forward ZPECB from 1a to 1d becomes 73.17 kJ/mol while the reverse ZPECB from 1f to 1d becomes 73.24 kJ/mol. The ZPECB from 1d to 1a is 14.92 kJ/mol and from 1d to 1f is 14.91 kJ/mol. The slight changes in absolute energies are in general not significant for order of magnitude rate constant calculations, but are responsible for the equilibrium isotopic fractionations (K_{eq}). For example, the zero-point corrected absolute energies of 1f are lower than 1a by ~0.08 kJ/mol, making it energetically more stable. Note that Xiao and Lasaga (1996) computed a ZPECB of 118 kJ/mol for an analogous reaction, where a hydrogen atom directly transfers from one OH group of H_4SiO_4 to another without the mediation of water molecules.

The intermediate 1d resembles the 5-coordinated silica species that have been previously modeled by Kubicki et al. (1993) and Xiao and Lasaga (1996). However, these modeled species were negatively charged ($H_5SiO_5^-$) in contrast to the neutral charge of our model. Sefcik and Goddard (2001), by accounting for hydration effects, have shown that the negatively charged species may not be stable relative to H_4SiO_4 in the aqueous phase. Kubicki (2001) in examining the protonation of H_4SiO_4 has shown that that a 5-coordinated intermediate may be formed in the presence of additional water molecules although this is for a more acidic system. Tacke et al. (2000) have successfully synthesized and isolated 5-coordinated silicon compounds with a SiO_5 skeleton but these synthetic compounds are stabilized by chelates and are bound in a crystalline matrix. Our absolute energies show that the aqueous 5-coordinated intermediate is much higher in energy compared to the corresponding reactants and products (1a or 1f) and is therefore relatively unstable. Furthermore, the low activation energy barriers from the intermediate to reactants or products may explain why 5-coordinated silica has yet to be observed in natural systems. In other words, our results indicate that an aqueous 5-coordinated silicon hydroxide is a short-lived intermediate in the presence of water; hence this explains why calculations show it is an energy minimum and yet it is an experimentally elusive species.

Solvation-corrected Gibbs free energies were computed using the implicit solvation method described above and Eqn. 4. The results are shown in Table 3. The pressures and dielectric constants were arbitrarily chosen using graphical curve fitting between 373K and 673K to coincide with pressure, temperature and dielectric constants used in Felipe et al. (2003). For 298K and $S_{vib} = 0$, the solvation corrected $\Delta G^{\ddagger}$ from 1a to 1d (or 1f to 1d) is 66.21 kJ/mol and the reverse direction is 12.06 kJ/mol. Upon substitution of ^{18}O in $O_{[1]}$, the solvation corrected $\Delta G^{\ddagger}$ from 1a to 1d decreases to 66.15 kJ/mol, whereas that from 1f to 1d increases to 66.22 kJ/mol. The solvation corrected $\Delta G^{\ddagger}$ from 1d to 1a is 12.05 kJ/mol, whereas that from 1d to 1f is 12.06 kJ/mol.

For 298K and $S_{vib} \neq 0$, the solvation corrected $\Delta G^{\ddagger}$ from 1a to 1d (or 1f to 1d) is 85.97 kJ/mol and is therefore much higher than that for $S_{vib} = 0$. The solvation corrected $\Delta G^{\ddagger}$ for the reverse direction is 20.41 kJ/mol and is also much higher than that for $S_{vib} = 0$. Thus, the exclusion of vibrational entropy ($S_{vib} = 0$), and presumably of large errors from internal rotational modes, decreases $\Delta G^{\ddagger}$ considerably.

Isotope exchange rates as inferred from NMR studies on dimerization and hydrolysis by Kinrade (1996) give free energies similar to our solvation corrected free energies with $S_{vib} = 0$. For example, at 298K, the experimental values of Kinrade (1996) yield $\Delta G^{\ddagger} = 70$ kJ/mol (from $\Delta H^{\ddagger} = 45$ kJ/mol and $\Delta S^{\ddagger} = -83$ J/K-mol). Thus, the predictions suggest that the reaction depicted in Figure 1 is slightly more favorable than exchange via dimerization/hydrolysis at 298K.

Enthalpies of activation for 298, 373, 473, 573 and 673K were predicted to be 65.9, 64.3, 62.5, 61.2 and 60.3 kJ/mol, respectively. Note that the activation enthalpy at 298K is higher than that measured by Kinrade (45 kJ/mol; 1996), even though

Table 4. Temperature-dependent rate constants computed using Eqn. 1 and Gibbs free energies from Table 3. Units are s^{-1}. Also shown are equilibrium constants computed using Eqn. 5.

T	k_1	k_{-1}	k_2	k_{-2}	k_{eq}
$\Delta S^{\ddagger}_{vib} = 0$					
298	1.60E+01	4.80E+10	4.80E+10	1.56E+01	1.027916
373	7.47E+03	2.20E+11	2.20E+11	7.33E+03	1.017067
473	1.21E+06	7.82E+11	7.81E+11	1.19E+06	1.008713
573	3.16E+07	1.77E+12	1.77E+12	3.14E+07	1.003864
673	3.17E+08	3.25E+12	3.25E+12	3.16E+08	1.001408
$\Delta S^{\ddagger}_{vib} \neq 0$					
298	5.39E−03	1.65E+09	1.65E+09	5.37E−03	1.006374
373	1.39E+00	5.35E+09	5.36E+09	1.39E+00	1.001694
473	1.37E+02	1.41E+10	1.41E+10	1.37E+02	0.998666
573	2.66E+03	2.63E+10	2.63E+10	2.67E+03	0.997249
673	2.21E+04	4.21E+10	4.22E+10	2.23E+04	0.996722

our mechanism is more favored in terms of the activation free energy. Thus, care must be taken when estimating the relative rates of reactions solely by activation enthalpies because the entropy of activation may contribute significantly to the activation free energy, and hence, the rate.

The pH dependence of experimental (and apparent) activation energies is often attributed to a protonation step that contributes 15–50 kJ/mol to the actual activation energies (Casey and Sposito, 1992). This contribution may therefore "contaminate" experimentally measured activation enthalpies. Hence, we compare our results only to related reactions with known pH independence. The predicted activation enthalpies were lower than experimental data for dissociating hydroxyl bridges of $Al_{13}O_4(OH)_{24}(H_2O)_{12}^{7+}$ (104 and 200 kJ/mol; Casey et al., 2000), and $GaAl_{12}O_4(OH)_{24}(H_2O)_{12}^{7+}$ (98 and 125 kJ/mol; Casey and Phillips, 2001), and for hydrolysis of oxygen bridges in dimers of Cr(III) (71–115 kJ/mol; Springborg, 1988). The activation enthalpies are also lower than pH independent hydrolysis of dimers in general (100–150 kJ/mol; see Springborg, 1988). The activation enthalpy is higher than oxygen exchange between $B(OH)_4^-$ and $B(OH)_3$ via a dimeric transition state (20.1 kJ/mol) and is within the activation enthalpy range of oxygen exchange between water and arsenic anions (25–92 kJ/mol) (Richens, 1997).

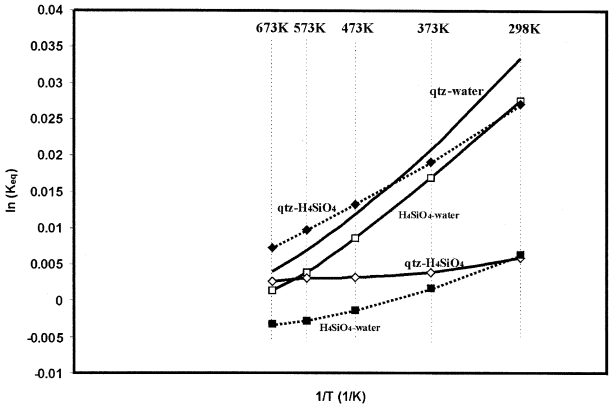

Fig. 3. Predicted and experimental equilibrium curves. The H_4SiO_4-water curves are calculated from B3LYP/6-31+G(d,p) data, and the qtz-water curve is from calcite and quartz curves of Clayton and Kieffer (1991) and calcite-water fractionation curves of O'Neil et al. (1969). The qtz-H_4SiO_4 curves are derived from the H_4SiO_4-water and qtz-water curves. Solid lines are for $\Delta S^{\ddagger}_{vib} = 0$, except for the qtz-water curve; dotted lines are for $\Delta S^{\ddagger}_{vib} \neq 0$. Squares are for the H_4SiO_4-water curves and diamonds are for the qtz-H_4SiO_4 curves.

4.3. Isotope Exchange Rate Constants

Using the ZPECBs computed and the vibrational frequencies from ab initio calculations, isotope exchange rate constants may be evaluated using Eqn. 1. The isotope exchange rates are shown in Table 4 for the following reactions:

$$H_4SiO_4 + H_2{}^{18}O + 6H_2O \rightarrow H_6SiO_4{}^{18}O + 6H_2O \qquad k_1 \quad (7)$$

$$H_6SiO_4{}^{18}O + 6H_2O \rightarrow H_4SiO_3{}^{18}O + 7H_2O \qquad k_2 \quad (8)$$

In the chosen temperature range and with $\Delta S^{\ddagger}_{vib} = 0$, the rate constants for k_1 or k_{-2} are about four orders of magnitude higher than the rate constants with $\Delta S^{\ddagger}_{vib} \neq 0$. In the temperature range, the rate constants for k_2 or k_{-1} are about two orders of magnitude higher than the rate constants with $\Delta S^{\ddagger}_{vib} \neq 0$. The data for $\Delta S^{\ddagger}_{vib} = 0$ and $\Delta S^{\ddagger}_{vib} \neq 0$ indicate that the reactions are reasonably fast. For any sequential two-step reaction, the rate is governed by the slower step. Hence, k_1 and k_{-2} are the rate-determining steps for the forward and reverse reactions, respectively.

At 298K for $\Delta S^{\ddagger}_{vib} = 0$ calculations, the half-life for the molecular complex at the right hand side of Eqn. 7 is 0.04 s, and the half-life of the C2 symmetric 5-coordinated intermediate 10^{-11} s. Hence, the extremely short half-life predicts the elusiveness of the 5-coordinated silica in solution. The predicted half-lives at 298K for the $\Delta S^{\ddagger}_{vib} \neq 0$ calculations are longer. The molecular complex has a half-life of 129 s, whereas the C2 intermediate has a half-life of 10^{-10} s. Thus, rates computed with the exclusion of errors from vibrational entropy ($S^{\ddagger}_{vib} = 0$), and presumably of large errors from internal rotational modes, indicate a much faster reaction rate. The half-life computed from the oxygen exchange via the dimerization/hydrolysis mechanism (Kinrade, 1996) is 0.18 s at 298K, and is higher than the half-life when entropy is excluded and lower than that when entropy is excluded. Hence, if neglect of vibrational entropy gives more accurate rate constants, then the results show that oxygen exchange is more predominantly due to the direct exchange of water and orthosilicic acid than due to dimerization/hydrolysis.

4.4. Isotope Exchange Equilibrium Constants

The isotope exchange equilibrium constants are shown in Table 4 and illustrated in Figure 3. At the chosen temperature range of 298K to 673K and for $\Delta S^{\ddagger}_{vib} = 0$, the fractionation factor $\alpha_{H4SiO4\text{-}H2O}$ decreases from 1.028 to 1.001. At the same temperature range and for $\Delta S^{\ddagger}_{vib} \neq 0$, $\alpha_{H4SiO4\text{-}H2O}$ decreases from 1.007 to 0.999; extending the range to 1573K shows $\alpha_{H4SiO4\text{-}H2O}$ increases back up asymptotically to 1.0 beginning at ~800K.

There are no known equilibrium studies of oxygen exchange between water and orthosilicic acid although the fractionation between water and quartz has been the subject of several studies (Clayton et al., 1972; Bottinga and Javoy, 1973; Becker and Clayton, 1976). For example, using the calcite and quartz curves of Clayton and Kieffer (1991) and the calcite-water fractionations of O'Neil et al. (1969), the quartz-water fractionation factors $\alpha_{qtz\text{-}H2O}$ are computed to be 1.034, 1.021, 1.012, 1.007 and 1.004 for 298K, 373K, 473K, 573K and 673K respectively (Fig. 3). This indirect method for calculating $\alpha_{qtz\text{-}H2O}$ was used because it is believed (Chacko et al., 2001) that this method does not incorporate salt effects in contrast to direct quartz-water methods (e.g., Clayton et al., 1972).

The experimental quartz-water equilibrium constants at the corresponding temperatures are consistently higher than our results in Table 4. For $S_{vib} = 0$, the difference between $\alpha_{qtz\text{-}H2O}$ and $\alpha_{H4SiO4\text{-}H2O}$ range from 0.003 to 0.006. For $S_{vib} \neq 0$, the difference is larger and range from 0.007 to 0.030. The results show that the exclusion of errors from the vibrational entropy ($S_{vib} = 0$) shifts the $\alpha_{H4SiO4\text{-}H2O}$ curve higher and closer to $\alpha_{qtz\text{-}H2O}$.

The similarity between the curves of $\alpha_{qtz\text{-}H2O}$ and $\alpha_{H4SiO4\text{-}H2O}$ (for $S_{vib} = 0$) is encouraging. The discrepancy was expected because the exchange between water and orthosilicic acid mainly involves hydroxide groups of orthosilicic acid, whereas the exchange between water and quartz involve mostly bridging oxygen atoms. From the MO-TST calculated $\alpha_{H4SiO4\text{-}H2O}$, and the experimental $\alpha_{qtz\text{-}H2O}$, a prediction can be made on $\alpha_{qtz\text{-}H4SiO4}$. The $\alpha_{qtz\text{-}H4SiO4}$ values are predicted to be 1.006 1.004 1.003 1.003 1.003 at 298K, 373K, 473K, 573K and 673K, respectively (Fig. 3). In other words, the fractionation between quartz and orthosilicic acid (and concomitantly, the amorphous surface layer) is expected to be much less than that between orthosilicic acid and water.

5. CONCLUSIONS

MO-TST calculations indicate that oxygen isotope exchange between water and H_4SiO_4 may occur through a two-step concerted proton transfer reaction. Therefore, similar to hydrogen exchange, the mobility of protons facilitates the exchange of oxygen. The reaction intermediate of the two-step mechanism is a symmetric 5-coordinated neutral silicon species that is relatively higher in energy than either the reactant or the product. Other alternative paths from this intermediate are energetically less favored paths. Our results show that the participation of water molecules in the transfer of protons lowers the ZPECB (and thus the activation energy) when compared with the ZPECB of oxygen exchange without the mediation of water molecules (Xiao and Lasaga, 1994). Rate constant calculations indicate that the 5-coordinated species has an extremely short half-life.

The isotope exchange reaction is expected to occur at rates sufficiently fast that equilibrium in most natural aqueous systems may be assumed. Equilibration occurs within a second at 298K according to the more accurate calculations. The fractionation factors computed are lower than, but close to, fractionation factors between mineral quartz and water and indicate that fractionation between quartz and $H_4\ SiO_{4(aq)}$ should be relatively small.

Acknowledgments—The authors are grateful for the support of the National Science Foundation (NSF EAR-9628238 and EAR-9727134) and the Department of Energy (DE-FG02-01ER15216 and DE-FG02-90ER14153). JDK thanks the support of the U.S. Department of Energy, Office of Basic Energy Sciences, Division of Chemical Sciences, Geosciences and Biosciences, under the project "Nanoscale Complexity at the Oxide-Water Interface" and by NSF grant EAR-0073722. Special thanks to Julian Tirado-Rives for clarification on the handling of free energies in the gaussian 98 output. The authors would specially want to thank the two reviewers and Bill Casey for their careful evaluation, excellent advice and numerous references.

Associate editor: W. H. Casey

REFERENCES

Ayala P. Y. and Schlegel H. B. (1998) Identification and treatment of internal rotation in normal mode vibrational analysis. *J. Chem. Phys.* **108,** 2314–2325.

Barker P. A., Street-Perrott F. A., Leng M. J., Greenwood P. B., Swain D. L., Perrott R. A., Telford R. J., and Ficken K. J. (2001) A 14,000-year oxygen isotope record from diatom silica in tow alpine lakes on Mt. Kenya.. *Science* **292,** 2307–2310.

Becke A. D. (1993) A new mixing of Hartree-Fock and local density-functional theories. *J. Chem. Phys.* **92,** 1372–1377.

Becker R. H. and Clayton R. N. (1976) Oxygen isotope study of a precambrian banded iron-formation, Hamersley Range, Western-Australia. *Geochim. Cosmochim. Acta* **40,** 1153–1165.

Bolton E. W., Lasaga A. C., and Rye D. M. (1999) Long-term flow/chemistry feedback in a porous medium with heterogeneous permeability: Kinetic control of dissolution and precipitation. *Am. J. Sci.* **299,** 1–68.

Bottinga Y. and Javoy M. (1973) Comments on oxygen isotope geothermometry. *Earth Planet. Sci. Lett.* **20,** 250–265.

Boys S. F. and Bernardi F. (1970) Calculation of small molecular interactions by differences of separate total energies—Some procedures with reduced errors. *Mol. Phys.* **19,** 553–566.

Brandriss M. E., O'Neil J. R., Edlund M. B., and Stoermer E. F. (1998) Oxygen isotope fractionation between diatomaceous silica and water. *Geochim. Cosmochim. Acta* **62,** 1119–1125.

Brasch N. E., Buckingham D. A., Bram Evans A., and Clark C. R. (1996) ^{17}O NMR study of chromium(VI) ions in water. *J. Am. Chem. Soc.* **118,** 7969–7980.

Cancès E., Mennucci B., and Tomasi J. (1997) A new integral equation formalism for the polarizable continuum model: Theoretical background and applications to isotropic and anisotropic dielectrics. *J. Chem. Phys.* **107,** 3032–3041.

Casey W. H. (2001) A view of reactions at mineral surfaces from the aqueous phase. *Min. Mag.* **65,** 323–337.

Casey W. H., Lasaga A. C., and Gibbs G. V. (1990) Mechanisms of silica dissolution as inferred from the kinetic isotope effect. *Geochim. Cosmochim. Acta* **54,** 3369–3378.

Casey W. H. and Sposito G. (1992) On the temperature dependence of mineral dissolution rates. *Geochim. Cosmochim. Acta* **56,** 3825–3830.

Casey W. H., Phillips B. L., Karlsson M., Nordin S., Nordin J. P., Sullivan D. J., and Neugebauer-Crawford S. (2000) Rates and mechanisms of oxygen exchanges between sites in the $AlO_4Al_{12}(OH)_{24}(H_2O)_{12}^{7+}$(aq) complex and water: Implications for

mineral surface chemistry. *Geochim. Cosmochim. Acta* **64,** 2951–2964.

Casey W. H. and Phillips B. L. (2001) Kinetics of oxygen exchange between sites in the $GaO_4Al_{12}(OH)_{24}(H_2O)_{12}{}^{7+}$(aq) molecule and aqueous solution. *Geochim. Cosmochim. Acta* **65,** 705–714.

Chacko T., Cole D. R., Horita J. (2001) Equilibrium oxygen, hydrogen and carbon isotope fractionation factors applicable to geologic systems. In *Stable Isotope Geochemistry* (eds. J.W. Valley and D. Cole). *Rev. Min. Geoch.***43,** 1–81.

Chiba H., Chacko T., Clayton R. N., and Goldsmith J. R. (1989) Oxygen isotope fractionations involving diopside, forsterite, magnetite, and calcite—Application to geothermometry. *Geochim. Cosmochim. Acta* **53,** 2985–2995.

Clayton R. N., Mayeda T. K., and O'Neil J. R. (1972) Oxygen isotope-exchange between quartz and water. *J. Geophys. Res.* **77,** 3057–3067.

Clayton R. N., Mayeda T. K., Goldsmith J. R., Chiba H., and Chacko T. (1988) Oxygen isotope fractionation factors among rock-forming minerals at high-temperatures. *Chem. Geol.* **70,** 183–183.

Clayton R. N., Goldsmith J. R., and Mayeda T. K. (1989) Oxygen isotope fractionation in quartz, albite, anorthite and calcite. *Geochim. Cosmochim. Acta* **53,** 725–733.

Clayton R. N. and Kieffer S. W. (1996) Oxygen isotopic thermometer calibrations. In *Stable Isotope Geochemistry: A Tribute to Samuel Epstein* (eds. H. P. Taylor, J. R. O'Neil, and I. R. Kaplan), pp. 3–10. Geochemical Society, San Antonio.

Cole D. R. (2000) Isotopic exchange in mineral-fluid systems. IV. The crystal chemical controls on oxygen isotope exchange rates in carbonate-H_2O and layer silicate-H_2O systems. *Geochim. Cosmochim. Acta* **64,** 921–931.

De Almeida W. B. and O'Malley P. J. (1991) The vibrational-spectrum of H_4SiO_4 calculated using ab initio molecular-orbital methods. *J. Mol. Struct.* **246,** 179–184.

Dove P. M. and Rimstidt JD. (1994) Silica-water interactions. In *Silica: Physical Behavior, Geochemistry and Materials Applications* (eds. PJ Heaney, CT Prewitt and GV Gibbs). *Rev. Min.***29**, 259–308.

Drenth W. and Kwart H. (1980) *Kinetics Applied to Organic Reactions*. Dekker.

East A. L. L. and Radom L. (1997) Ab initio statistical thermodynamical models for the computation of third-law entropies. *J. Chem. Phys.* **106,** 6655–6674.

Felipe M. A., Xiao Y and Kubicki JD. (2001) Molecular orbital modeling and transition state theory in geochemistry. In *Molecular Orbital Modeling and Transition State Theory: Applications in the Geosciences.* (eds. RT Cygan and JD Kubicki). *Rev. Min. Geoch.***42**, 485–531.

Felipe M. A., Kubicki J. D., and Rye D. M. (2003) Hydrogen isotope exchange kinetics between H_2O and H_4SiO_4 from ab initio calculations. *Geochim. Cosmochim. Acta* **67,** 1259–1276.

Foresman J. B. and Frisch A. (1996) *Exploring Chemistry with Electronic Structure Methods*. Gaussian.

Frisch M. J., Trucks G. W., Schlegel H. B., Scuseria G. E., Robb M. A., Cheeseman J. R., Zakrzewski V. G., Montgomery J. A., Stratmann R. E., Burant J. C., Dapprich S., Millam J. M., Daniels A. D., Kudin K. N., Strain M. C., Farkas O., Tomasi J., Barone V., Cossi M., Cammi R., Mennucci B., Pomelli C., Adamo C., Clifford S., Ochterski J., Petersson G. A., Ayala P. Y., Cui Q., Morokuma K., Malick D. K., Rabuck A. D., Raghavachari K., Foresman J. B., Cioslowski J., Ortiz J. V., Stefanov B. B., Liu G., Liashenko A., Piskorz P., Komaromi I., Gomperts R., Martin R. L., Fox D. J., Keith T. A., Al-Laham M. A., Peng C. Y., Nanayakkara A., Gonzalez C., Challacombe M., Gill P. M. W., Johnson B. G., Chen W., Wong M. W., Andres J. L., Head-Gordon M., Replogle E. S. and Pople JA. (1998) Gaussian 98 (Revision A7). Gaussian.

Frisch M. J., Trucks G. W., Schlegel H. B., Gill P. M. W, Johnson B. G., Robb M. A., Cheeseman J. R., Keith T. A., Petersson G. A., Montgomery J. A., Raghavachari K., Al-Laham M. A., Zakrzewski V. G., Ortiz J. V., Foresman J. B., Cioslowski J., Stefanov B. B., Nanayakkara A., Challacombe M., Peng C. Y., Ayala P. Y., Chen W., Wong M. W., Andres J. L., Replogle E. S., Gomperts R., Martin R. L., Fox D. J., Binkley, J. S., Defrees D. J., Baker J., Stewart J. P., Head-Gordon M., Gonzalez C. and Pople JA (1995) Gaussian 94 (Revision D1). Gaussian, Inc. Pittsburgh.

Geissler P. L., Dellago C., Chandler D., Hutter J., and Parrinello M. (2001) Autoionization in liquid water. *Science.* **291,** 2121–2124.

Gotze J., Tichomirowa M., Fuchs H., Pilot J., and Sharp Z. D. (2001) Geochemistry of agates: A trace element and stable isotope study. *Chem. Geol.* **175,** 523–541.

Hehre W. J., Ditchfield R., and Pople J. A. (1972) Self-consistent molecular orbital methods. XII. Further extension of Gaussian-type basis sets for use in molecular orbital studies of organic molecules. *J. Chem. Phys.* **56,** 2257–2261.

Hehre W. J., Radom P. R., and Pople J. A. (1986) *Ab Initio Molecular Orbital Theory*. Wiley.

Iler R. K. (1979) *The Chemistry of Silica*. Wiley.

Jenkin G. R. T., Craw D., and Fallick A. E. (1994) Stable isotopic and fluid inclusion evidence for meteoric fluid penetration into an active mountain belt—Alpine Schist, New-Zealand. *J. Metamorph. Geol.* **12,** 429–444.

Jia Y. F., Li X., and Kerrich R. (2001) Stable isotope (O, H, S, C, and N) systematics of quartz vein systems in the turbidite-hosted Central and North. Deborah gold deposits of the Bendigo cold field, Central Victoria, Australia: Constraints on the origin of ore-forming fluids. *Econ. Geol. Bull. Soc.* **96,** 705–721.

Keutsch F. N. and Saykally R. J. (2001) Water clusters. Untangling the mysteries of the liquid, one molecule at a time. *Proc. Nat. Acad. Sci. USA* **98,** 10533–10540.

Kinrade S. D. (1996) Oxygen-17 NMR study of aqueous potassium silicates. *J. Phys. Chem.* **100,** 4760–4764.

Knauth L. P. (1994) Petrogenesis of chert. In *Silica: Physical Behavior, Geochemistry and Materials Applications* (eds. PJ Heaney, CT Prewitt and GV Gibbs). *Rev. Min.***29**, 233–258.

Knight C. T. G., Thompson A. R., Kunwar A. C., Gutowsky H. S., Oldfield E., and Kirkpatrick R. J. (1989) O-17 nuclear magnetic-resonance spectroscopic studies of aqueous alkaline silicate solutions. *J. Chem. Soc. Dalton Trans.* **2,** 275–281.

Kobko N. and Dannenberg J. J. (2001) Effect of basis set superposition error (BSSE) upon ab initio calculations of organic transition states. *J. Phys. Chem. A* **105,** 1944–1950.

Kubicki J. D. (2001) Self-consistent reaction field calculations of aqueous Al^{3+}, Fe^{3+}, and Si^{4+}: Calculated aqueous-phase deprotonation energies correlated with experimental In(K-a) and pK(a). *J. Phys. Chem. A* **105,** 8756–8762.

Kubicki J. D., Xiao Y., and Lasaga A. C. (1993) Theoretical reaction pathways for the formation of $[Si(OH)_5]^{1-}$ and the deprotonation of orthosilicic acid in basic solution. *Geochim. Cosmochim. Acta* **57,** 3847–3853.

Lasaga A. C. and Rye D. M. (1993) Fluid-flow and chemical-reaction kinetics in metamorphic systems. *Am. J. Sci.* **293,** 361–404.

Lee C. T., Yang W. T., and Parr R. G. (1988) Development of the Colle-Salvetti correlation-energy formula into a functional of the electron-density. *Phys. Rev. B* **37,** 785–789.

Lee A .P., Phillips B. L., and Casey W. H. (2002) Kinetics of oxygen exchange between the $GaO_4Al_{12}(OH)_{24}(H_2O)_{12}{}^{7+}$(aq) molecule and aqueous solution. *Geochim. Cosmochim. Acta* **66,** 577–587.

Lobaugh J. and Voth G. A. (1996) The quantum dynamics of an excess proton in water. *J. Chem. Phys.* **104,** 2056–2069.

Luth K. and Scheiner S. (1992) Calculation of barriers to proton-transfer using multiconfiguration self-consistent-field methods (1) effects of localization. *J. Chem Phys.* **97,** 7507–7518.

Martin D. and Duprez D. (1996) Mobility of surface species on oxides. 1. Isotopic exchange O-18(2) with O-16 of SiO_2, Al_2O_3, ZrO_2, MgO, CeO_2, and CeO_2-Al_2O_3. Activation by noble metals. Correlation with oxide basicity. *J. Phys. Chem.* **100,** 9429–9438.

McMillan P. F. and Hess A. C. (1990) Ab initio valence force-field calculations for quartz. *Phys. Chem. Min.* **17,** 97–107.

Newton MD. and Gibbs GV. (1980) Ab initio calculated geometries and charge-distributions for H_4SiO_4 and $H_6Si_2O_7$ compared with experimental values for silicates and siloxanes. *Phys. Chem. Min.* **6,** 221–246.

O'Neil J. R. (1986) Theoretical and experimental aspects of isotopic fractionation. In *Stable Isotopes*(eds. JW Valley, HP Taylor Jr., and JR O'Neil). *Rev. Min.* **16,** 1–40.

O'Neil J. R., Clayton R. N., and Mayeda T. K. (1969) Oxygen isotope fractionation in divalent metal carbonates. *J. Chem. Phys.* **51,** 5547–5558.

Pelmenschikov A. G., Morosi G., and Gamba A. (1997) Adsorption of water and methanol on silica hydroxyls: Ab initio energy and frequency calculations. *J. Phys. Chem. A* **101,** 1178–1187.

Peng C. and Schlegel H. B. (1994) Combining synchronous transit and quasi-newton methods for finding transition states. *Israel J. Chem.* **33,** 449–454.

Phillips B. L., Casey W. H., and Karlsson M. (2000) Bonding and reactivity at oxide mineral surfaces from model aqueous complexes. *Nature* **404,** 379–382.

Pople J. A., Scott A. P., Wong M. W., and Radom L. (1993) Scaling factors for obtaining fundamental vibrational frequencies and zero-point energies from HF/6–31+G* and MP2/6–31+G* harmonic frequencies. *Israel J. Chem.* **33,** 345–350.

Richens D. T. (1997) *The Chemistry of Aqua Ions*. Wiley.

Rimstidt J. D. and Barnes H. L. (1980) The kinetics of silica-water reactions. *Geochim. Cosmochim. Acta* **44,** 1683–1699.

Sauer J. (1989) Molecular-models in ab initio studies of solids and surfaces—From ionic-crystals and semiconductors to catalysts. *Chem. Rev.* **89,** 199–255.

Schmidt M., Botz R., Stoffers P., Anders T., and Bohrmann G. (1997) Oxygen isotopes in marine diatoms: A comparative study of analytical techniques and new results on the isotope composition of recent marine diatoms. *Geochim. Cosmochim. Acta* **61,** 2275–2280.

Schmidt M., Botz R., Rickert D., Bohrmann G., Hall S. R., and Mann S. (2001) Oxygen isotopes of marine diatoms and relations to opal-A maturation. *Geochim. Cosmochim. Acta* **65,** 201–211.

Scott A. P. and Radom L. (1996) Harmonic vibrational frequencies: An evaluation of Hartree-Fock, Møller-Plesset, quadratic configuration interaction, density functional theory, and semiempirical scaling factors. *J. Phys. Chem.* **100,** 16502–16513.

Sefcik J. and Goddard W. A. (2001) Thermochemistry of silicic acid deprotonation: Comparison of gas-phase and solvated DFT calculations to experiment. *Geochim. Cosmochim. Acta* **65,** 4435–4443.

Shemesh A., Rietti-Shati M., Rioual P., Battarbee R., de Beaulieu J. L., Reille M., Andrieu V., and Svobodova H. (2001) An oxgyen isotope record of lacustrine opal from a European Maar indicates climatic stability during the last interglacial. *Geophys. Res. Lett* **28,** 2305–2308.

Springborg J. (1988) Hydroxo-bridged complexes of chromium(III), cobalt(III), rhodium(III) and iridium(III). *Adv. Inorg. Chem.* **32,** 55–169.

Swaddle T. W. (2001) Silicate complexes of aluminum(III) in aqueous systems. *Coord. Chem. Rev* **219-221,** 665–686.

Tacke R., Burschka C., Richter I., Wagner B., and Willeke R. (2000) Pentacoordinate silicon compounds with SiO_5 skeletons containing SiOH or SiOSi groups: Derivatives of the pentahydroxosilicate^{1-} anion $[Si(OH)_5]$ $[(HO)_4Si\text{-}O\text{-}Si(OH)_4]^-$ and its anhydride $[Si(OH)_5]$ $[(HO)_4Si\text{-}O\text{-}Si(OH)_4]^{2-}$. *J. Am. Chem. Soc.* **122,** 8480–8485.

Webb J. A. and Golding S. D. (1998) Geochemical mass-balance and oxygen isotope constraints on silcrete formation and its paleoclimatic implications in Southern Australia. *J. Sed. Res.* **68,** 981–993.

Webb E. A. and Longstaffe F. J. (2000) The oxygen isotopic compositions of silica phytoliths and plant water in grasses: Implications for the study of paleoclimate. *Geochim. Cosmochim. Acta* **64,** 767–780.

Williams L. B., Hervig R. L., and Bjorlykke K. (1997) New evidence for the origin of quartz cements in hydrocarbon reservoirs revealed by oxygen isotope micro analyses. *Geochim. Cosmochim. Acta* **61,** 2529–2538.

Xiao Y. T. and Lasaga A. C. (1994) Ab-initio quantum-mechanical studies of the kinetics and mechanisms of silicate dissolution—$H^+(H_3O^+)$ catalysis. *Geochim. Cosmochim. Acta* **58,** 5379–5400.

Xiao Y. T. and Lasaga A. C. (1996) Ab initio quantum mechanical studies of the kinetics and mechanisms of quartz dissolution: OH^- catalysis. *Geochim. Cosmochim. Acta* **60,** 2283–2295.

Zotov N. and Keppler H. (2002) Silica speciation in aqueous fluids at high pressures and high temperatures. *Chem. Geol.* **184,** 71–82.